Surface Science 628 (2014) 1–7

Contents lists available at ScienceDirect

Surface Science

journal homepage: www.elsevier.com/locate/susc

Ab-initio study of the structural, electronic and optical properties of BSb (110) and (100) surfaces

Hojat Allah Badehian *,[1], Hamdollah Salehi

Department of Physics, Shahid Chamran University, Ahvaz, Islamic Republic of Iran

ARTICLE INFO

Article history:
Received 21 February 2014
Received in revised form 30 April 2014
Accepted 5 May 2014
Available online 13 May 2014

Keywords:
DFT
Surface energies
Work functions
Surface relaxation
Band structures
Optical properties

ABSTRACT

In the present study, the structural, electronic and optical properties of BSb bulk, BSb (110) and (100) surfaces were investigated. The calculations were performed by using Full-Potential Linear Augmented Plane Wave (FP-LAPW) in Density Functional Theory (DFT) framework with various exchange-correlation functionals. Some surface properties such as surface energies, the work functions, surface relaxation, band structures and optical properties of cubic BSb (110) and (100) nano-slabs were studied. The (100) surface of cubic BSb has B- and Sb-terminations while the (110) surface has only one termination. The surface properties of all the terminations were presented and discussed. Moreover, some bulk properties such as structural, electronic, band structure and optical properties of BSb compound were investigated for comparison. The obtained band gap for the BSb (110) nano-slab was 0.38 eV while the BSb (100) nano-slab showed a metallic behavior. Moreover, the surface states of the slabs were identified. The real and imaginary parts of the dielectric function of the BSb (110) nano-slab were also calculated and compared with bulk results.

1. Introduction

The group III–V semiconductors are widely used for electronic and optoelectronic tools. [1]. Among these compounds, the narrow band gap antimonide based compound semiconductors (ABCS) are widely considered as the first candidate materials for production of the third generation infrared photon detectors and ICs with ultra-high speed and ultra-low power consumption. Due to their unique band gap structure and physical properties, it makes a wide space to develop new varied devices [2]. However, III-Sb compounds have attracted more attention due to their potential usage in rechargeable lithium batteries. Among III-Sb compounds, boron antimonide exhibits a strong covalent character and shows an uncommon behavior because of small core and lack of "p" electrons in boron atom compared to other group III–V compounds. It makes this material a potential material for high temperature electronic and optical application [3]. The surfaces of group III–V semiconductors have a fundamental importance because their cleanness, geometry and photoelectric properties deeply affect the function of modern electronic devices [4]. The (110) nonpolar surface of III–V compounds has been broadly investigated and more concentration has been on their relaxed geometry, phonon vibrations and band structure [5–9]. Surface energy and work function are two important parameters for fully recognizing the surfaces [9,10]. Nowadays, various surfaces of group III–V compounds are developing owing to their applications in thin films. Regarding the fact that thin film process technology is firmly linked to the basic investigations on the surfaces and interfaces, their fundamental parameters including surface energy and work function must be specified first. Although they have wide applications, due to their difficulties in measurements few investigations are available [11–13]. Surface energy is defined as the difference of free energy between a surface atom and that of an inner one for a solid which is one of the most fundamental properties for expressing surfaces stabilities [14]. In the most experimental works, surface energy is achieved by extrapolating the value of liquid surface energies at high temperatures which give rise to less valid experimental data [15]. Another important property of surfaces is work function which was first introduced by Einstein when he was working on the photoelectric effect and is expressed as minimum required work to separate free electron from the inner of a solid away from the surface into the vacuum region [16]. Kelvin probe is proper device to calculate work function values from contact potential difference between the surface under study and a standardized surface [16,17]. Although this process is simple and nondestructive the work function value is easily affected by impurities, roughness and misorientation on the surfaces [18]. Some other issues such as polycrystallinity of the sample and absence of required ideal vacuum also lower the accuracy in experiments [12]. Regarding the abovementioned complications that occur in calculating the surface energy and work function in experimental studies, we believe that

* Corresponding author.
E-mail addresses: hojatbadehian@gmail.com (H.A. Badehian), salehi_h@scu.ac.ir (H. Salehi).
[1] Tel.: +98 9177314414.

http://dx.doi.org/10.1016/j.susc.2014.05.002
0039-6028/

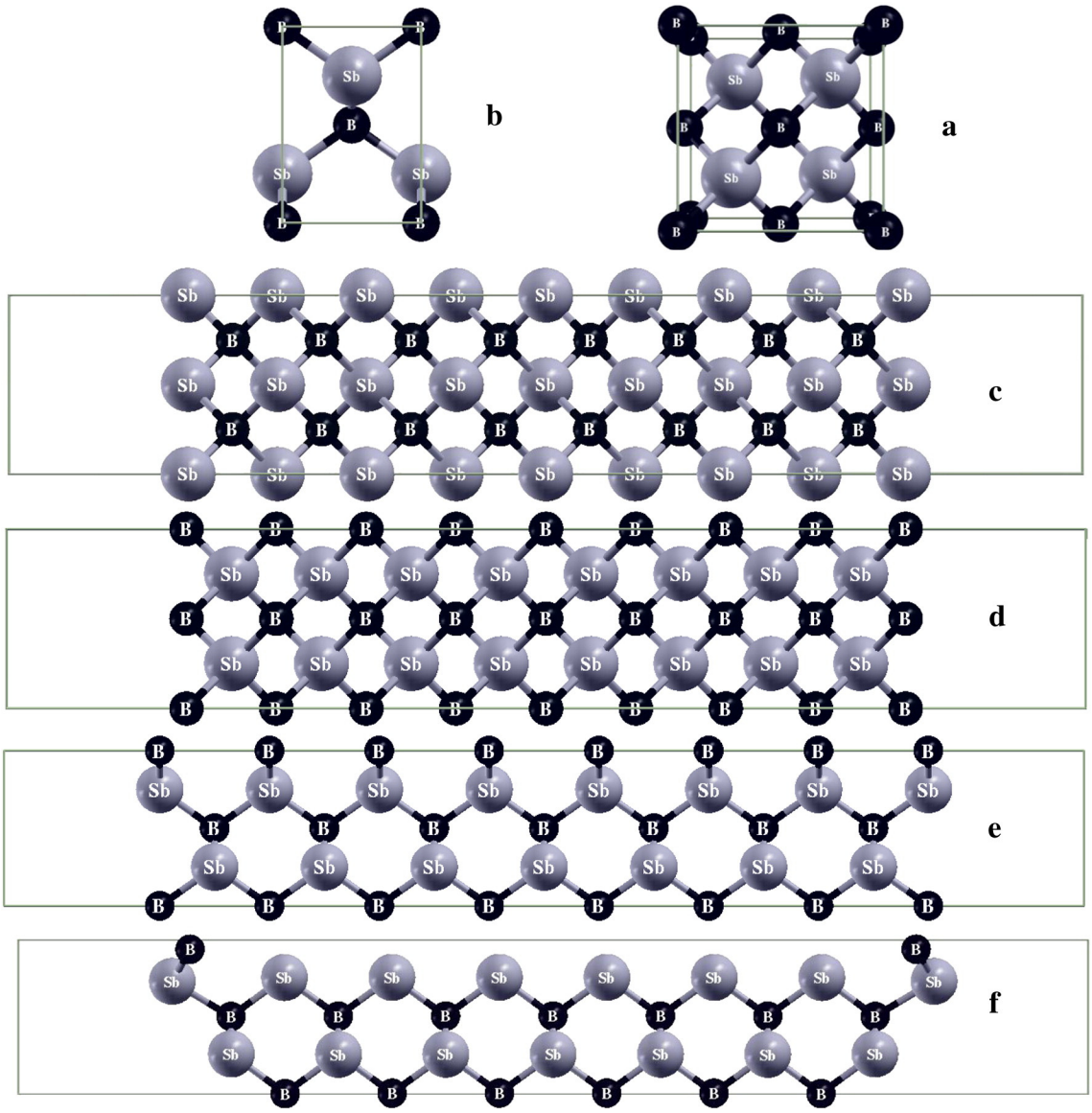

Fig. 1. (a) Bulk unit cell of BSb, (b) the top view of the BSb (110) slab, (c) symmetric 17 layer BSb (100) slab in the *z* direction (Sb-termination), (d) symmetric 17 layer BSb (100) slab in the *z* direction (B-termination), (e) symmetric 15 layer BSb (110) slab and (f) fully relaxed symmetric 15 layer BSb (110) slab.

theoretical studies can overcome these deficiencies. Over the last few decades, surface energy and work function of some pure elements and many other compounds have been calculated using DFT method. Most of the investigations on the BSb compound have been theoretical. Bagci and et al. reported pseudopotential study of structural, electronic and vibrational properties of the BSb (110) surface in 2008 [19]. To the

Table 1
Calculated lattice constant, a_0 (Å), bulk modulus, B_0 (GPa) and its pressure derivative B' of the BSb compound in the ZB phase using different functionals.

Approximations	**a**(**Å**)	**B**(**GPa**)	**B′**(**GPa**)
GGA-PBE	5.2809	98.9264	4.7660
LDA	5.1954	115.0498	5.0570
PBEsol	5.2316	108.2133	4.9070
WU-Chen	5.2354	107.7334	4.8818
Other results	5.278[a], 5.279[b], 5.278[c], 5.191[d], 5.201[e], 5.145[f], 5.21[g], 5.252[h], 5.177[i]	100[a], 96[b], 100[c], 111[d], 116[e], 118[f], 110[g], 103[h], 110[i]	4.40[a], 4.55[b], 4.40[c], 4.36[d], 4.16[e], 4.31[f], 4.07[g], 3.62[h], 4.237[i]

[a] FP-GGA Ref. [28].
[b] FP-GGA Ref. [3].
[c] FP-GGA Ref. [29].
[d] FP-LDA Ref. [3].
[e] FP-LDA Ref. [29].
[f] PP-GGA Ref. [30].
[g] PP-GGA Ref. [31].
[h] FP-GGA Ref. [32].
[i] FP-GGA Ref. [33].

Table 2
Atomic displacements in the upper three layers on the (110) surface along the *z* axes; values are both in Å.

Layers	Atoms	Δz (Å)
I	B	−0.4215
	Sb	+0.19815
II	B	+0.0091
	Sb	−0.0085
III	B	−0.0159
	Sb	+0.0200

best of our knowledge, there is no work reporting surface energy, work function and optical properties of BSb (110) and (100) surfaces; therefore, we weren't able to compare our findings with other results.

2. Computational approach

FP-LAPW method within the density functional theory, implemented in the WIEN2k code [20], has been applied to investigate the structural, electronic and optical properties of BSb bulk, BSb (110) and (100) surfaces. Local density approximation (LDA), generalized gradient approximation Perdew–Burke–Ernzerhof (GGA-PBE) [21] and modified Becke–Johnson functionals (mBJ-GGA) [22] approximation have been used for exchange and correlation energy terms.

In order to reach energy eigenvalue convergence, the wave functions in the interstitial region were expanded in plane waves with a cut-off $K_{max} = 8/R_{MT}$, where R_{MT} stands for the smallest atomic muffin-tin sphere radius and K_{max} is the magnitude of the largest K vector in the plane wave expansion. The valence wave functions inside the muffin-tin spheres are expanded up to $l_{max} = 10$, whereas the charge density was Fourier expanded up to $G_{max} = 14$ (a.u.)$^{-1}$. The self-consistent calculations are considered to be converged when the total energy of the system is stable within 10^{-5} Ryd. The integrals over the Brillouin zone are performed up to 54 k-points in the irreducible Brillouin zone, using the Monkhorst–Pack special k-point approach [23]. The energy which separates the valence state from the core state has been considered −6.0 Ryd. In the calculations $5s^2\ 4d^{10}\ 5p^3$ and $2s^2\ 2p^1$ states behaved as valence electrons for Sb and B respectively. BSb (100) and (110) slabs were constructed using an optimized bulk structure obtained from PBE-GGA approximation. An artificial periodicity along the *z* direction perpendicular to the surface was applied in the simulations. The same values as the bulk calculations were considered for K_{max}, R_{MT}, l_{max} and G_{max}. The Monkhorst–Pack k-point mesh of $15 \times 10 \times 1$ for integration over the Brillouin zone (BZ) was used for BSb (110) slabs and $15 \times 15 \times 1$ mesh for BSb (100) slabs. BSb (100) and (110) surfaces are modeled by the supercell technique of (1×1) unit cell using symmetric slabs of 17 and 15 atomic layers respectively and the vacuum of 20 Bohr was considered for both slabs. It is essential to provide enough vacuum between layers of compounds so that the electrostatic interactions between two sides of a slab are negligible and electrostatic potential reaches its asymptotic value. In Fig. 1, schematic plots of bulk structure, unrelaxed BSb (110) and BSb (100) slabs and fully relaxed BSb (110) slab are depicted.

For the B-terminated surface, the unit slab consists of nine B and eight Sb layers, so that the slab is terminated with the B layer on either surface. For the Sb-terminated slab, there are eight B and nine Sb layers in the unit slab, so we have a slab with Sb layers terminated on both outmost surfaces. During the surface structure optimization, we attempted top 3–5 layers for the relaxation, it is found that the differences both in the B – Sb bond length and the distance between the surface and subsurface atoms are very small. Namely, the differences of the B – Sb bond length are less than 0.002 Å. So, the relaxation of the top four layers for the two typical slabs is adequate to study the surface properties.

Table 3
Atomic displacements in the upper three layers on the (100) surface along the *z* axes in both B- and Sb-terminations; values are both in Å.

Layers	Terminations	Δz (Å)
I	B	−0.4550
	Sb	+0.3802
II	B	−0.1555
	Sb	+0.1717
III	B	−0.1838
	Sb	+0.1303

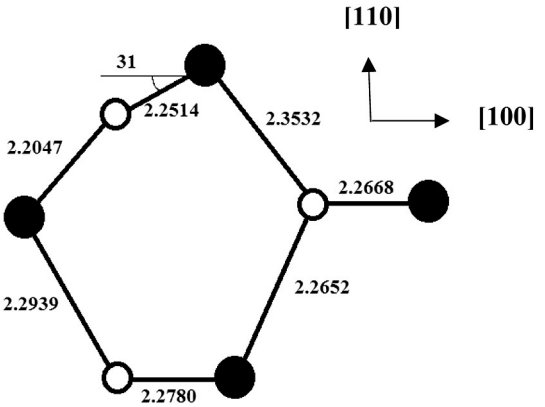

Fig. 2. Schematic view of the BSb (110) relaxed structure along with bond length.

3. Results

3.1. Structural properties of the bulk

The structural properties of BSb were obtained by optimizing total energy. The total energies were calculated for the different volumes around the equilibrium cell volume V_0. Then, they are fitted to Murnaghan's equation of state [24] to determine the ground state properties such as the equilibrium lattice constant a_0, the bulk modulus B and its pressure derivative. The calculated equilibrium parameters were found using different functionals listed in Table 1. This table also contains other theoretical data for comparison. It may be noted here that the LDA underestimates and GGA overestimates the experimental lattice parameter. These results are consistent with the general trends of the LDA and GGA approximations [25,26]. The calculated structural parameters show a good agreement with available literature values. According to the results of Table 1 and since GGA functionals give rise to a more accurate result for structural and electronic properties than other functionals [27], the rest of the calculations were performed using this functional.

3.2. Surface relaxations

In surface calculation, the decreasing of the interlayer distance between the first and second layers of atoms with respect to subsequent layers in the bulk is a rather dominant phenomenon. The surface may be thought of as an intermediate between a diatomic molecule and the bulk structure. Since the interatomic distances in diatomic molecules are much smaller than in the bulk, there is a rationale for the

Table 4
Surface energies and work functions of BSb (110) and BSb (100) by GGA-PBE.

Layers	σ (j/m^2)		φ (eV)	
	Relaxed	Unrelaxed	Relaxed	Unrelaxed
110	1.355	1.814	4.43	4.56
100 (Sb)	0.3172	0.3321	4.63	4.94
100 (B)	0.3122	0.3275	4.69	5.32

Table 5
Band gaps of BSb in bulk and surfacates.

Compound	GGA-PBE	mBJ-GGA	Other calculations
BSb (bulk)	0.741	1.190	0.75[a], 0.527[b], 0.844[c], 0751[d], 0.763[e], 1.334[f], 0.71[g], 0.56[h], 0.54[i], 0.51[j]
BSb (110)	0.20	0.38	–
BSb (100)	0	0	–

[a] FP-LAPW Ref. [43].
[b] PP-LDA Ref. [40].
[c] PP-GGA Ref. [41].
[d] FP-LDA Ref. [3].
[e] FP-GGA Ref.[3].
[f] FP-EVA Ref. [3].
[g] FP-GGA Ref. [29].
[h] FP-LDA Ref. [29].
[i] FP-GGA Ref.[42].
[j] PW-PP Ref. [33].

surface relaxation. This may be contrasted with reconstruction where the relaxation of atoms yields new surface primitive cells. In relaxation, the atoms maintain their structure in the surface plane as it was (according to the projection of the bulk cell on the surface); only their distance from the bulk changes [34]. In our simulations, the BSb (110) and (100) slabs are constructed based on the optimized bulk geometry obtained from GGA-PBE approximation. Each surface unit cell of the (110) consists of one cation and one anion with two broken bonds. After relaxations, it is expected that the atomic positions of the top layers of surfaces and the distances between first layers, deviate from bulk state. It can be a result of a rearrangement of broken covalent or ionic bonds at the surface. Under such conditions the atoms at the surface bunch into rows with alternately larger and smaller spacings than in the bulk. That is, for some crystals held together by valence bonds, creation of a surface would leave unsaturated bonds dangling into space. The energy may then be lowered if neighboring atoms approach each other and form bonds with their otherwise unused valence electrons [34]. Surface relaxation in DFT was done by minimization of total energy of supercell as a function of positions of the atoms, with only the atoms in the top layers allowed to move. The relaxed structures of (110) nano-slab are illustrated in Fig. 1. The surface relaxation of BSb (100) in B- and Sb terminations was small and relative positions of surface atoms didn't vary while the first three layer distances changed; however, the BSb (110) surface had a rumpling after relaxation. After the relaxation, the cations move inward while the anions move outward

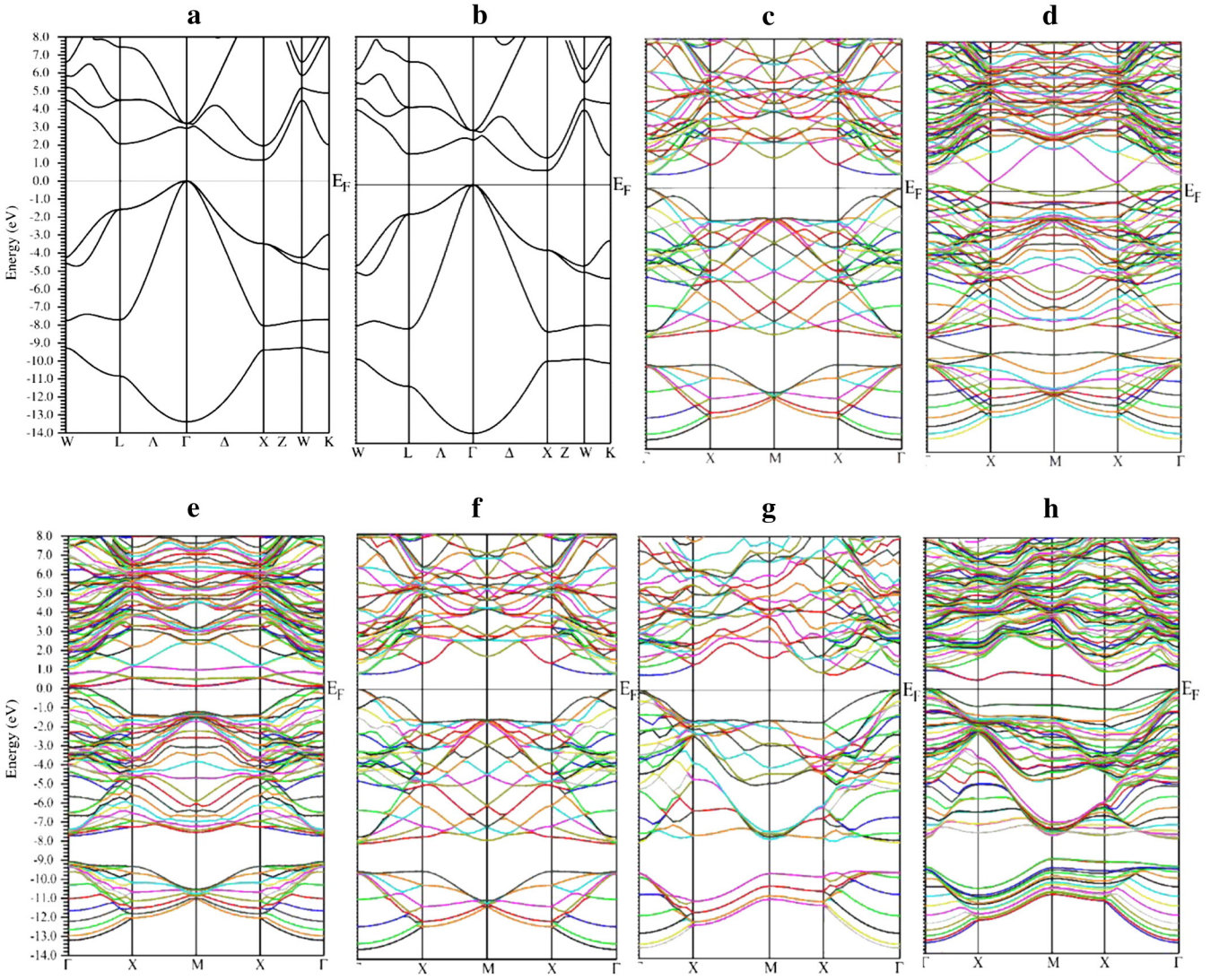

Fig. 3. Band structure profiles of (a) bulk BSb with mBJ, (b) bulk BSb with GGA-PBE, (c) bulk supercell for (100) Sb-termination with GGA-PBE, (d) BSb (100) Sb-termination slab with GGA-PBE, (e) BSb (100) B-termination slab with GGA-PBE, (f) bulk supercell for (100) B-termination with GGA-PBE, (g) bulk supercell for (110) slab with GGA and (h) BSb (110) slab with GGA-PBE.

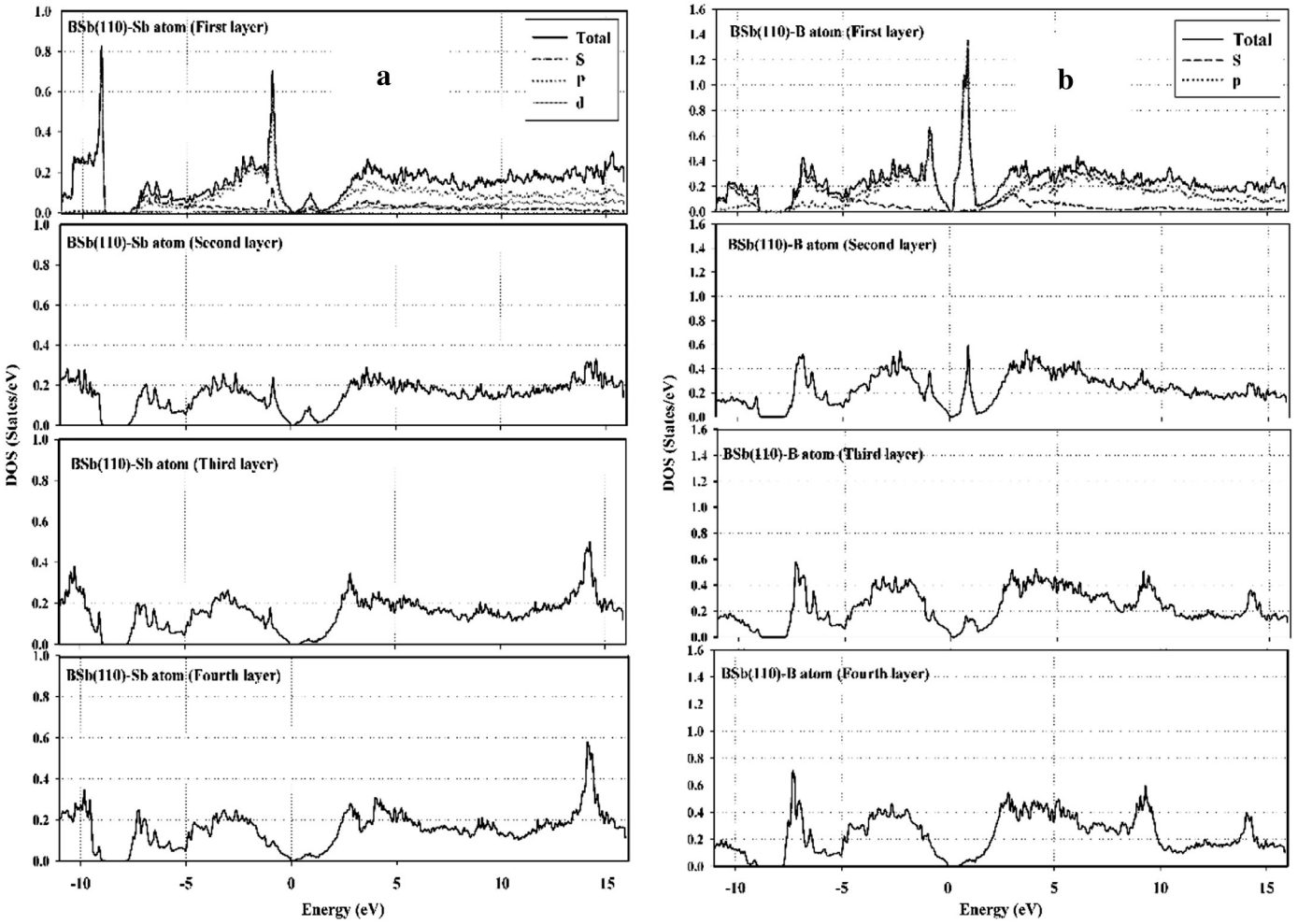

Fig. 4. The LDOS of the (a) Sb and (b) B atoms for the four outermost layers of the BSb (110).

owing to the charge transfer from the former to the latter. The relaxation of III–V (110) surfaces is well known: the cation–anion chains become tilted with the anions being raised [35]. The calculated structural parameters of the relaxed BSb (110) and (100) surfaces are given in Tables 2 and 3 respectively. From the results of these tables, one can see that displacements of atoms from regular lattice sites do not exceed 9% of bulk lattice constant. In deeper layers, the displacements of atoms from their crystalline positions are quickly decreasing. B atoms move only down along the *z*-axis and Sb atoms move only up along the *z*-axis. Consequently, the Sb ions at the surfaces sit above surface B ions with the 11% rumpling. The buckling (tilt) angle of the top layer for BSb (110) is found to be 31.1°, in agreement with Bagci work [19]. Bond length along with schematic view of the BSb (110) relaxed structure is shown in Fig. 2.

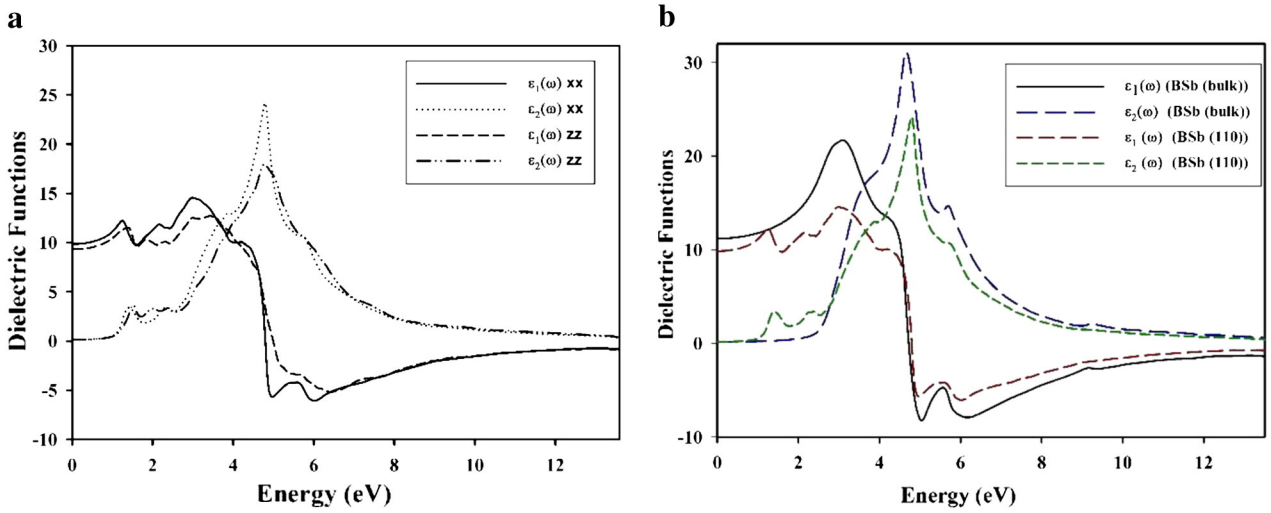

Fig. 5. The real and imaginary part of the dielectric function of (a) BSb bulk and BSb (110) slab in the *x* direction and (b) BSb (110) in the *x* and *z* directions.

Table 6
Calculated static dielectric function $\varepsilon_1(0)$ and static refractive function (n) in x, y and z directions with PBE and mBJ functionals.

Compound	Functionals	Directions	$\varepsilon_1(0)$	Static refractive index (n)
BSb (bulk)	GGA-PBE	x, y, z	11.19	3.35
	mBJ-GGA	x, y, z	8.47	2.91
Exp.	–	x, y, z	–	2.52 [42], 3.34 [45], 3.30 [30]
BSb (110)	GGA-PBE	x, y	9.85	3.14
		Z	9.39	3.06
	mBJ-GGA	x, y	7.70	2.77
		Z	7.32	2.71

Each surface anion has two bonds to surface cations and one back bond to a second layer cation; an analogous situation applies to the cations. Since the anion dangling bond is lower in energy than the cation dangling bond state [36] charge is transferred to lower the total energy. Thus the anion dangling bond state is completely filled, such that the surface, which would be metallic with a half filled anion and cation dangling bond band, becomes semiconducting. Because of the missing charge in the cation, this atom moves inward to arrive at a geometry which is closer to sp^2. This process causes a surface relaxation in which the symmetry of the surface is maintained, but the bond angles are changed because of rehybridization [37]. Therefore, the dangling bonds of the surface cations are empty while the dangling bonds of the surface anions are fully occupied. The first layer cations prefer to be bonded to their group-V nearest neighbors in a nearly planar sp^2 configuration while the first-layer anions prefer a p-bonding configuration with their group-III nearest neighbors.

3.3. Surface energy and work function BSb (110) and (100) surfaces

Surface energy and work function are two fundamental parameters in surface studies and the calculation of them requires the systems with high precision and is so costly in the experiment. In DFT calculations surface energy is determined as follows:

$$\sigma = \frac{1}{2A}\left(E_{slab} - NE_{bulk}\right) \tag{1}$$

where E_{slab} is the total energy of an N-layer slab calculated with a sufficient large value of N, E_{bulk} denotes the bulk energy, A is the surface of slab (top or down), and "2" in the denominator indicates that two surfaces are involved in the calculations due to three dimensional boundary conditions.

Work function is defined as an energy difference between a vacuum level E_{vac} and the Fermi energy E_F, which can be expressed as [38]:

$$\varphi = E_{VAC} - E_F \tag{2}$$

In DFT calculations, E_{vac} is the value of potential energy in the middle of vacuum and E_F represents Fermi energy. The calculated surface energies and work functions for relaxed and unrelaxed BSb (110) and BSb (100) were listed in Table 4. Unfortunately there is no theoretical and experimental work for comparing our finding with theirs. These results can be used in future investigations.

In order to estimate the surface energy of BSb (100), we start with the cleavage energy for unrelaxed B- and Sb-terminated surfaces. In our calculations the two 17 layer B- and Sb-terminated slabs represent together 34 bulk unit cells. Surfaces with both terminations arise simultaneously under cleavage of the crystal and the relevant cleavage energy is distributed equally between created surfaces. Thus, we consider that the cleavage energy is the same for both terminations [38]:

$$E_S^{(unrel)} = \frac{1}{4}\left[E_{slab}^{(unrel)}(B) + E_{slab}^{(unrel)}(Sb) - 34E_{bulk}(BSb)\right] \tag{3}$$

where $E_{slab}^{(unrel)}(B)$ and $E_{slab}^{(unrel)}(Sb)$ are unrelaxed B- and Sb-terminated slab energies, E_{bulk} is the energy per a bulk unit cell, and a factor of four arises from the fact that we construct four surfaces upon cleavage procedure. Next, we can calculate the (negative) relaxation energies for each of B and Sb terminations, when both sides of slabs relax:

$$E_{rel}(A) = \frac{1}{2}\left[E_{slab}^{(unrel)}(A) + E_{slab}^{(relaxed)}(A)\right] \tag{4}$$

E_{slab} (A) is a slab energy after relaxation, A = B or Sb. Lastly, the surface energy sought for is just a sum of the cleavage and relaxation energies

$$\sigma(A) = E_S^{(unrel)}(A) + E_{rel}(A) \tag{5}$$

The results of calculations for the surface energy of relaxed surfaces σ are presented in Table 4. In all calculations the σ values for B termination are slightly smaller than for the Sb termination. However, the energy difference is small and both surfaces are stable and energetically equally favorable.

3.4. Electronic properties

As mentioned above, most investigations done on the bulk and surface of BSb were theoretical and they have predicted that bulk BSb is a semiconductor with the indirect band gap of 0.5–1.3 eV [3,29,39–43]. In this work, the energy band structures of bulk BSb, BSb (110) and BSb (100) slabs were calculated using GGA-PBE and mBJ-GGA functionals. The results of the band gaps were presented in Table 5 and compared with other theoretical works. The findings are consistent with others. It is found that mBJ-GGA improved the band gap energy which is consistent with the general trend of this functional [22]. It is also obvious that the band gap of BSb (110) slab was decreased and the BSb (100) slab (B- and Sb-termination) had no gap showing metallic behavior. This is because the band gap of a surface narrows in comparison with the corresponding bulk value, and this change even leads to an insulator–metal transition when the corresponding bulk band gap value is small [17].

At the free surface of a semiconductor there often exist surface-bound electronic states with energies in the forbidden gap between the valence and conduction bands of the bulk semiconductor [44]. In order to identify the surface states, the band structure of bulk BSb supercells with the same structure and geometry of the slabs but without the vacuum, was calculated. By comparing the band structure profile of the bulk supercell and corresponding slabs, one can easily distinguish the surface states. The band structure profiles of the bulk, bulk supercells and the slabs are also illustrated in Fig. 3. The orbital character is attained from contributions of the different orbitals to the local density of states (LDOS). For the BSb (110), the lowest surface state in the conduction band corresponds mostly to the empty cation dangling sp^2 hybrid orbitals while the top surface state in the valence band corresponds mostly to the occupied anion 5p dangling orbitals. For the Sb-terminated of BSb (100), the surface states in the conduction band correspond mostly to the Sb 5p orbitals in the surface layer and the surface states in the valence band correspond mostly to the occupied anion 5p dangling orbitals. Moreover, in the case of the B-terminated BSb (100), the surface states in the fundamental gap correspond to the cation surface layer and have a p_z character. The LDOS of the B and Sb atoms for the four outermost layers of the BSb (110) slab were depicted in Fig. 4.

3.5. Optical properties

The optical properties of materials are one of the important matters in investigations and have several applications in industry. The optical properties of a solid can be characterized by complex dielectric functions $\varepsilon(\omega)$ which represent the linear response of the system to an

external electromagnetic field with a small wave vector. Having calculated this function, other optical properties can be obtained properly. $\varepsilon(\omega)$ can be expressed as:

$$\varepsilon(\omega) = \varepsilon_1(\omega) + i\varepsilon_2(\omega) \tag{6}$$

The imaginary part of dielectric function is calculated by:

$$\varepsilon_2(\omega) = \left(\frac{4\pi^2 e^2}{m^2\omega^2}\right)\sum\int (\langle i|M|j\rangle)^2 f_i(1-f_i) \times \delta\left(E_f - E_i - \omega\right) d^3k \tag{7}$$

where M is the dipole matrix, i and j the initial and final states, respectively, f_i the Fermi distribution function for the ith state and E_i the energy the electron in the ith state. The real part of dielectric function is also obtained from $\varepsilon_2(\omega)$ by Kramers–Kroning relation:

$$\varepsilon_1(\omega) = 1 + \frac{2}{\pi}P\int_0^{\infty} \frac{\omega'\varepsilon_2(\omega')d\omega'}{\left(\omega'^2 - \omega^2\right)} \tag{8}$$

where P is the principal value of the integral.

In this work, the real and imaginary parts of the dielectric function of BSb bulk and BSb (110) nano-slab were calculated and compared to each other. The results are illustrated in Fig. 5. As it is expected, the general shape of the imaginary and real parts of the dielectric function of bulk and the slab are roughly the same. Moreover, one can see some peaks (close to 1 eV) in the beginning of dielectric function of BSb (110) slab spectrum. The peaks are raised due to the transitions to the surface states. Since the slabs are symmetric in the x and y directions, therefore the dielectric function in these directions is similar. Consequently, the optical properties of the slab were investigated in the x and z directions (Fig. 5-b). The static dielectric function, $\varepsilon_1(0)$, for bulk BSb is about 11.19 and for BSb (110) slab in the x and z directions are 9.85 and 9.39 respectively. As a result, the calculated static refractive index ($n = \sqrt{\varepsilon_1(0)}$) for the bulk BSb is about 3.35 and for BSb (110) slab in x and z directions is 3.14 and 3.06 respectively. The results listed in Table 6 are in good agreement with other available data.

4. Conclusion

In this work, the structural, electronic and optical properties of the BSb compound in bulk phase and surface phase ((100) and (110) surfaces) were investigated using the FP-LAPW approach in the DFT framework with various functionals. The two B- and Sb-temination of BSb (100) surface were studied and compared with bulk and the (110) surface. The structural properties of the bulk BSb such as equilibrium lattice constant, bulk modulus and its first pressure derivative were calculated and discussed. The obtained results are consistent with others results. The relaxation of three first layers of BSb (110) and (100) (both termination) surfaces were also investigated. No surface reconstruction was detected for all slabs. The surface relaxation of BSb (100) in B- and Sb terminations was small and the relative positions of surface atoms didn't vary while the first three layer distances changed; however, the BSb (110) surface had a rumpling after relaxation. The tilt angle of the top layer of the BSb (110) surface was found to be 31.1°. Moreover, the surface energy and work function of these surfaces, both in relaxed and unrelaxed states, were calculated. In addition, the band structure of BSb bulk and the slabs was studied and the surface states were determined. Besides, the dielectric function, static dielectric constant and refractive index of BSb bulk and BSb (110) slab were obtained and compared with each other. Overall, our results are consistent with available data.

Acknowledgments

I would like to express my very great appreciation to my brother Dr. Ziaedin Badehian for his valuable and constructive suggestions during the editing of this research work. His willingness to give his time so generously has been very much appreciated.

References

[1] S. Adachi, Handbook on Physical Properties of Semiconductors, Kluwer Academic Publishers, 2004.
[2] C. Liu, Y. Li, Y. Zeng, Engineering 2 (2010) 617.
[3] A. Rashid, E.A. Fazal, S.J. Hashemifar, R. Haris, H. Akbarzadeh, Commun. Theor. Phys. 52 (2009) 527.
[4] P. Ebert, Surf. Sci. Rep. 33 (1999) 121.
[5] H.M. Tütüncü, G.P. Srivastava, Phys. B Condens. Matter 263–264 (1999) 400.
[6] H. Nienhaus, Phys. Rev. B 56 (1997) 13194.
[7] N. Esser, K. Hinrichs, J.R. Power, W. Richter, J. Fritsch, Phys. Rev. B 66 (2002) 075330.
[8] H. Nienhaus, W. Mönch, Phys. Rev. B 50 (1994) 11750.
[9] N. Ooi, J.B. Adams, Surf. Sci. 574 (2005) 269.
[10] W. Liu, X. Liu, W.T. Zheng, Q. Jiang, Surf. Sci. 600 (2006) 257.
[11] Q. Jiang, H.M. Lu, M. Zhao, J. Phys. Condens. Matter 16 (2004) 521.
[12] H.L. Skriver, N.M. Rosengaard, Phys. Rev. B 46 (1992) 7157.
[13] D.L. Price, B.R. Cooper, J.M. Wills, Phys. Rev. B 48 (1993) 15311.
[14] Q. Jiang, D.S. Zhao, M. Zhao, Acta Mater. 49 (2001) 3143.
[15] G. Renaud, Surf. Sci. Rep. 32 (1998) 5.
[16] W. Li, D.Y. Li, J. Chem. Phys. 122 (2005) 064708.
[17] W. Liu, W.T. Zheng, Q. Jiang, Phys. Rev. B 75 (2007) 235322.
[18] D.Y. Li, W. Li, Appl. Phys. Lett. 79 (2001) 4337.
[19] S. Bagci, S. Duman, H.M. Tütuncü, G.P. Srivastava, J. Phys. Conf. Ser. 100 (2008) 072013.
[20] K.S.P. Blaha, G. Madsen, D. Kvasnika, K. Luitz, WIEN2k, an augmented plane wave plus local orbitals program for calculating crystal properties, in, Vienna—Austria, 2001.
[21] J.P. Perdew, K. Burke, M. Ernzerhof, Phys. Rev. Lett. 77 (1996) 3865.
[22] F. Tran, P. Blaha, Phys. Rev. Lett. 102 (2009) 226401.
[23] H.J.M.a.J.D. Pack, Phys. Rev. B 13 (1976) 5188.
[24] F.D. Murnaghan, PNAS 30 (1944) 244.
[25] R.K.A. Bouhemadou, M. Kharoubi, T. Seddik, Ali H. Reshak, Y. Al-Douri, Comput. Mater. Sci. 45 (2009) 474.
[26] D. Heciri, L. Beldi, S. Drablia, H. Meradji, N.E. Derradji, H. Belkhir, B. Bouhafs, Comput. Mater. Sci. 38 (2007) 609.
[27] M. Ernzerhof, G.E. Scuseria, J. Chem. Phys. 110 (1999) 5029.
[28] D. Strauch, BSb: elastic coefficients, internal strain parameter, in: U. Rössler (Ed.), New Data and Updates for IV–IV, III–V, II–VI and I–VII Compounds, their Mixed Crystals and Diluted Magnetic Semiconductors, Springer, Berlin Heidelberg, 2011, p. 270.
[29] H. Meradji, S. Drablia, S. Ghemid, H. Belkhir, B. Bouhafs, A. Tadjer, Phys. Status Solidi B 241 (2004) 2881.
[30] S. Cui, W. Feng, H. Hu, Z. Feng, Phys. Status Solidi B 246 (2009) 119.
[31] E. Deligoz, K. Colakoglu, Y.O. Ciftci, J. Phys. Chem. Solids 68 (2007) 482.
[32] F.E.H. Hassan, H. Akbarzadeh, M. Zoaeter, J. Phys. Condens. Matter 13 (2004) 293.
[33] S.Q. Wang, H.Q. Ye, Phys. Rev. B 66 (2002) 235111.
[34] C. Kittel, Introduction to Solid State Physics, Wiley, 1971.
[35] H.M. Tütüncü, G.P. Srivastava, Phys. Rev. B 59 (1999) 4925.
[36] J. Pollmann, P. Krüger, Chapter 2 Electronic structure of semiconductor surfaces, in: K. Horn, M. Scheffler (Eds.), Handbook of Surface Science, North-Holland, 2000, p. 93.
[37] K. Horn, Electronic Structure, Elsevier Science, 2000.
[38] E. Heifets, R.I. Eglitis, E.A. Kotomin, J. Maier, G. Borstel, Phys. Rev. B 64 (2001) 235417.
[39] B. Bouhafs, H. Aourag, M. Certier, J. Phys. Condens. Matter 12 (2000) 5655.
[40] M. Ferhat, B. Bouhafs, A. Zaoui, H. Aourag, J. Phys. Condens. Matter 10 (1998) 7995.
[41] D. Xiong, S. Zhou, Q. Wang, L. Luo, Y. Huang, X. Ren, Sci. China Ser. G Phys. Mech. Astron. 52 (2009) 843.
[42] A. Zaoui, S. Kacimi, A. Yakoubi, B. Abbar, B. Bouhafs, Phys. B Condens. Matter 367 (2005) 195.
[43] B. Bachir, H. Aourag, M. Certier, J. Phys. Condens. Matter 12 (2000) 5655.
[44] C. Kittel, Introduction to Solid State Physics, 8th edition Wiley, 2004.
[45] S. Labidi, H. Meradji, S. Ghemid, S. Meçabih, B. Abbar, J. Optoelectron. Adv. Mater. 11 (2009) 994.